Excess fibronectin 1 participates in pathogenesis of pre-eclampsia by promoting apoptosis and autophagy in vascular endothelial cells

Haiying Wu, Kan Liu, Jingli Zhang

Obstetrical department, Henan Provincial People's Hospital, People's Hospital of Zhengzhou University, Zhengzhou, Henan Province, China.

Correspondence to: Haiying Wu

E-mail:Haiying1968@outlook.com

Address: Obstetrical Department, Henan Provincial People's Hospital, No.7 Weiwu Road, Zhengzhou, 450003, Henan Province,China. ORCID: 0000-0002-1822-8180

Tel:+8613503713179.

Running title: Plasma fibronectin 1 and pre-eclampsia

Abstract

Plasma fibronectin 1 (FN1) levels are elevated in individuals with pre-eclampsia (PE), which may be applied as a possible biochemical marker for vascular endothelial injury during PE. In the present study, the possible role of FN1 in the pathogenesis of PE and regulation of apoptosis and autophagy in vascular endothelial cells was explored. Plasma FN1 levels in 80 patients with PE and 40 healthy pregnant individuals were measured using ELISA to verify its relationship with the severity of PE. pcDNA3.1-FN1 or FN1-small interfering (si) RNA was used to manipulate the expression of FN1 in human umbilical vein endothelial cells (HUVECs) to assess the effects of FN1 on cell apoptosis, autophagy and the phosphoinositide 3-kinase (PI3K)/protein kinase B (AKT)/ mechanistic target of rapamycin (mTOR) signaling pathway. It was found that upregulation of FN1 promoted apoptosis and autophagy, in addition to significantly inhibiting the activation of AKT and mTOR in HUVECs. By contrast, downregulation of FN1 expression inhibited cell apoptosis and autophagy, but increased AKT and mTOR phosphorylation in HUVECs that were cultured in serum samples obtained from patients with PE. Rescue experiments found that the PI3K/AKT inhibitor LY294002 reversed the effects of FN1-siRNA on apoptosis and autophagy in HUVECs cultured in serum from patients with PE. Therefore, data from the present study suggest that FN1 participates in the pathogenesis of PE by promoting apoptosis and autophagy in vascular endothelial cells, which is associated with the PI3K/AKT/mTOR signaling pathway.

Key words: fibronectin1; plasma; pre-eclampsia; pathogenesis; vascular endothelial cells; apoptosis; autophagy; phosphoinositide 3-kinase/protein kinase B/mechanistic target of rapamycin

Introduction

Pre-eclampsia (PE) is a complex multisystem disorder that is characterized by the presence of hypertension and proteinuria after 20 weeks of pregnancy (Rana, *et al*.,2019). It is one of the most common causes of neonatal disease and perinatal death, accounting for 5%–8% worldwide (Witcher,2018; Gathiram and Moodley,2016). The pathogenesis of PE is highly complex and remains to be fully elucidated. A number of previous studies have reported that systemic endothelial dysfunction is the fundamental mechanism underlying the pathogenesis of PE (Osol, *et al*.,2017; Ali and Khalil,2015). At present, endothelial cellular injury is a research hotspot in the study of PE pathogenesis. It has been reported that the dysregulation of endothelial cell apoptosis is involved in each step of PE pathogenesis, as is autophagy (Nakashima, *et al*.,2017; Levy,2005). Up-regulation of alpha-actinin-4 (ACTN4) significantly inhibited endothelial cell apoptosis through regulating the p38-mitogen activated protein kinase/p53 pathway in PE (Zhao, *et al*.,2019). Furthermore, adverse factors, such as those involved in angiogenesis , can potentially exist in the maternal and fetal circulation during PE, which can result in endothelial cell damage to limit the function of the vascular endothelium (de Alwis, *et al*.,2020; Monte, *et al*.,2020).

Fibronectin 1 (FN1) is a glycoprotein that is involved in cellular adhesion and cell diffusion, and is widely distributed in healthy membranes, vessel structures and smooth-muscle cell layers (Speziale, *et al*.,2019). There exist two forms of FN1: soluble and insoluble. Plasma FN1 is a soluble protein that is synthesized and secreted primarily by hepatocytes and vessel endothelial cells (He, *et al*.,2015). Plasma FN1 has been shown to be upregulated under the setting of vascular tissue damage, inflammation and various diseases, including ischaemic heart disease and clear cell renal carcinoma (To and Midwood,2011; Yokomizo, *et al*.,2011). By contrast, insoluble FN1 is synthesized by fibroblasts and macrophages and alters the properties of the extracellular matrix and regulates cellular processes downstream (He, *et al*.,2015; To and Midwood,2011). Several studies have suggested that plasma FN1 can serve as a marker of endothelial damage (Aydin, *et al*.,2006). In particular, levels of plasma FN1 are reported to be elevated in individuals with PE, suggesting plasma FN1 as a potentially valuable marker for the prediction of PE (Dogan, *et al*., 2014; Jones, *et al*.,1996). This is supported by observations that elevated plasma FN1 can serve as a possible biochemical marker for vascular endothelial injury and dysfunction during PE (Yang, *et al*.,2018). Zhao *et al*. (2017) previously suggested that FN1, FBJ murine osteosarcoma viral oncogene homolog (FOS), and integrin alpha5 (ITGA5) may promote the development of PE by regulating differentiation, apoptosis, and invasion of human extravillous trophoblasts. Therefore, it is hypothesized that reducing the expression of FN1 may be a target for the prevention of endothelial dysfunction in PE. However, the number of reports studying the

potential role and mechanism of FN1 action in vascular endothelial cell physiology remains low.

In the present study, the level of plasma FN1 in pregnant women with PE was measured to determine if a correlation between FN1 and PE pathogenesis exists. Subsequently, human umbilical vein endothelial cells (HUVECs) were cultured with serum obtained from patients with PE to mimic the internal environment during PE and to explore the mechanistic effects of FN1 on HUVECs apoptosis and autophagy.

Materials and Methods

Subjects

In total, 80 pregnant women who were diagnosed with PE in Henan Provincial People's Hospital from Jan, 2016 to Jan, 2019, were assigned to the mild PE (MP; n=48), and severe PE (SP; n=32) groups, according to the Diagnosis Guidelines in ACOG Committee on Practice Bulletins-Obstetrics (2002). The following inclusion criteria were used: met the PE diagnostic criteria as specified in classification, diagnosis and management of the hypertensive disorders of pregnancy from the International Society for the Study of Hypertension in Pregnancy (Tranquilli, *et al*.,2014); singleton pregnancy; patients were aged >18 years; gestational age at enrollment was 20–34 weeks; no medical history of other pregnancy complications, including liver or renal diseases. In addition, 40 healthy pregnant women (20–34 gestational weeks at enrollment) were randomly recruited at Henan Provincial People's Hospital from Jan, 2016 to Jan, 2019 and designated as the control group.

There was no difference in age, gestational age or BMI at enrollment among individuals in the MP, SP and control groups (Table I). All study processes were performed in accordance with The Declaration of Helsinki. All participants signed the informed consent and the present study was approved by the Ethical Committee of Henan Provincial People's Hospital.

ELISA

Fasting peripheral venous blood (3 ml) was collected from all participants at the time of enrollment (20-34 gestational weeks) using citrate as an anticoagulant. The plasma was separated by centrifugation at 1 000 g for 10 min at -4℃ and stored at -80 °C. Plasma FN1 was examined using a human FN1 ELISA kit (EF1045-1, Assaypro, Missouri, USA), according to the manufacturer's instructions.

Cell culture

Primary HUVECs were purchased from Cell Bank of Type Culture Collection of the Chinese Academy of Science. All cells were cultured in EGM-2 medium (Gibco, Thermo fisher Scientific, Waltham, USA) supplemented with 10% fetal bovine serum (FBS; Gibco, Thermo fisher Scientific, Waltham, USA) in an incubator at 37 °C with 5% CO_2. HUVECs were sub-cultured after reaching 80%–90% confluence. The fourth generation of HUVECs was used for the subsequent experiments.

Grouping and transfection

Samples of fasting peripheral venous blood (2 ml) were collected from 10 healthy pregnant individuals and 10 patients with SP, who were selected at random from their respective groups. After standing for 1 h at room temperature, serum was isolated by centrifugation at 2 000 g for 15 min at -4 ℃. Serum was collected and subjected to filtration and sterilization. After heat-inactivation, the serum was aliquoted in 1.5 ml Eppendorf tubes and stored at -80 °C for subsequent cell culture.

The pcDNA3.1-FN1 and pcDNA3.1 empty vectors, FN1-small interfering (si) RNA and the corresponding negative control (NC) were purchased from Shanghai GenePharma Co., Ltd, China. HUVECs in the logarithmic growth phase were seeded into 6-well plates and divided into the following groups: Blank (cultured with 10% FBS); pcDNA3.1-FN1 (cultured with 10% FBS and transfected with pcDNA3.1-FN1), pcDNA3.1-NC (cultured with 10% FBS and transfected with pcDNA3.1 empty vector), Control (cultured with 10% serum from healthy pregnant women), PE (cultured with 10% serum from patients with PE), NC-siRNA (cultured with 10% serum from patients with PE and transfected with NC-siRNA), FN1-siRNA (cultured with 10% serum from patients with PE and transfected with FN1-siRNA), and LY294002 (MedChemExpress, Shanghai, China) +FN1-siRNA (cultured with 10% serum from patients with PE and 10 μM LY294002 [phosphoinositide 3-kinase (PI3K) inhibitor], then transfected with FN1-siRNA). The cells were transfected using lipofectamine 2000 or RFect siRNA transfection Reagent (11012, Baidai, Changzhou, China) at 70% confluence. Reverse transcription-quantitative PCR (RT-qPCR) and

western blotting were performed to measure the level of FN1 protein to verify the transfection efficiency after 24 or 48 h transfection.

RT-qPCR

Total RNA in cells was extracted using Trizol (Invitrogen, Thermo Fisher Scientific, Waltham, USA) and the cDNA was synthesized using a SuperScript First Strand cDNA reverse transcription kit (Invitrogen, Thermo Fisher Scientific, Waltham, USA), according to the manufacturer's instructions. Primers were synthesized by Sangon Biotech Co., Ltd, and the sequences were as follows: FN1, sense: 5'-GCTGACAGAGAAGATTCCCG-3', antisense: 5'-CCAGGGTGATGCTTGGAGAA-3'; GAPDH, sense: 5'-GGCCACTAGGCGCTCAC-3', antisense: 5'-CAAATCCGTTGACTCCGACC-3'. The RT-qPCR analyses were performed using a Rotor-Gene SYBR Green PCR kit (Qiagen, Duesseldorf, Germany) and the thermocycling conditions were performed as follows: 95°C for 10 min; followed by 40 cycles of 95°C for 10 sec and 60°C for 15 sec. The relative mRNA expression level of FN1 was calculated using the $2^{-\Delta\Delta Ct}$ method with GAPDH as an internal reference.

TUNEL assay

The HUVECs were seeded on coverslips in 6-well plates. The cells were washed with PBS and fixed with 4% paraformaldehyde at room temperature for 15 min. After washing with PBS, the cells were treated with proteinase K solution. The protocols were performed strictly as described in the TUNEL Assay kit-BrdU-Red (Abcam,

Cambridge, UK): TUNEL reaction solution was prepared and added to cells, prior to incubation at 37°C for 1 h in the dark. After being washed with PBS, the cells were staining with DAPI for 10 min, and rinsed again with PBS. Anti-fluorescent quenching mounting medium (Boster, Wuhan, China) was added for sealing. The numbers of apoptotic cells, which were stained with red-blue fluorescence, were observed under a fluorescence microscope at 200 times magnification.

Detection of autophagosome formation with Ad-mCherry-GFP-LC3B

HUVECs at the logarithmic growth phase in each group were cultured in 24-well plates for 24 h at 37℃, and infected with the adenovirus expression mCherry-green fluorescent proteins-LC3B fusion protein (Ad-mCherry-GFP-LC3B) (Beyotime Institute of Technology, Shanghai, China) at a multiplicity of infection (MOI) of 40 for 24 h at 37°C. Yellow or red dots were observed under a laser scanning confocal microscope (Leica Microsystems, Wetzlar, Germany) at 1 000 times magnification to evaluate autophagosome formation and autophagosome maturation into autolysosomes.

Western blotting

Total proteins were extracted from HUVECs in each group according to the protocol for the ProtoPrep® Total Extraction Sample Kit (Sigma-Aldrich, MA, USA). Protein concentrations were measured using bicinchoninic acid method (Beyotime Institute of Technology, Shanghai, China). Samples of 40 μg protein were separated by 10% sodium dodecyl sulphate–polyacrylamide gel electrophoresis and transferred onto

polyvinylidene fluoride (PVDF) membranes (EMD Millipore, USA). The membranes were blocked for 1 h in TBST with 5% skimmed milk and incubated with primary antibodies (Abcam, Cambridge, UK): FN1(1:1000), B cell lymphom/lewkmia-2 (Bcl-2) (1:1000), Bcl-2 associated X protein (Bax) (1:2000), cysteinyl aspartate specific proteinase-9 (Caspase-9) (1:1000), autophagy related gene 5 (ATG5) (1:1000), Beclin-1 (BECN1) (1:2000), microtubule associated protein 1 light chain 3 beta (LC3B) (1:3000), protein kinase B (Akt) (1:1000), AKT with phospho T308 (p-Akt) (1:1000), mechanistic target of rapamycin (mTOR) (1:1000), mTOR with phospho S2448 (p-mTOR) (1:1000), and GAPDH (1:5000) at 4℃ overnight. The following secondary antibodies: horseradish peroxidase-labeled goat anti-mouse or goat anti-rabbit IgG (1:5000) were incubated for 1 h. The protein bands were visualized using an enhanced chemiluminescence detection reagent (Sangon Biotech, Shanghai, China) and the relative expression was calculated using Image J software (National Institutes of Health, New York, USA) with GAPDH as the loading control.

Statistical analysis

All data were analyzed with SPSS Statistics v21.0 (IBM Corp, New York, USA). Measurement data was represented by means±SD. Differences between the two groups were analyzed using Student's *t*-test or ANOVA, followed by a least significant difference *t* test for multiple group comparisons. $P<0.05$ was considered to indicate a statistically significant difference.

Results

Levels of plasma FN1 in patients with PE

Plasma FN1 levels, measured by ELISA, are shown in Fig. 1. The levels of FN1 in patients in the PE group as a whole, including patients with MP and SP, were significantly higher compared with those in patients in the control group ($P<0.05$). In addition, FN1 levels in patients in the MP group was lower compared with those in patients in the SP group ($P<0.05$), suggesting that plasma FN1 may associate with the pathogenesis and severity of PE.

Expression of FN1 in HUVECs

The morphology of HUVECs was observed under a microscope (Fig. 2A). It was observed that HUVECs in the blank and control groups arranged in around a central point, while the cells in the PE group were arranged sparsely, with poorly defined boundaries between the nuclei and cytoplasm.

The expression level of FN1 in HUVECs transfected with pcDNA3.1-FN1 or FN1-siRNA was detected by RT-qPCR and western blotting (Fig. 2B and C, Supplementary Fig. S1). There was no difference in the level of FN1 mRNA and protein between cells in the blank and control groups, but the FN1 was up-regulated in the pcDNA3.1-FN1 group compared with the pcDNA3.1-NC group, suggesting that the FN1 was overexpressed in the HUVECs transfected with pcDNA3.1-FN1. In addition, FN1 was up-regulated in HUVECs cultured in serum from patients with PE,

compared with that in the blank and control groups. Furthermore, the expression of FN1 in cells in the FN1-siRNA group was significantly lower compared with that in the NC-siRNA group, suggesting that FN1-siRNA downregulated the expression of FN1 in HUVECs cultured with serum from patients with PE.

Effect of FN1 overexpression and knockdown on HUVECs apoptosis

The TUNEL assay was used to investigate the effect of FN1 on apoptosis in HUVECs (Fig. 3). The results showed that there was no difference in the apoptotic rate between the blank (15.48±3.15%) and control groups (17.69±3.54%). The apoptotic rate in the PE group was (50.37±4.75%), which is higher compared with that in the control group. The apoptotic rate in the pcDNA3.1-FN1 group (40.67±5.73%) was higher compared with that in the pcDNA3.1-NC group (16.97±3.42%). By contrast, the apoptotic rate in the FN1-siRNA group (24.83±3.76%) was lower compared with that in the NC-siRNA group (51.87±5.12%). Furthermore, the downstream marker proteins were detected by western blotting (Fig. 4A, Supplementary Fig. S2). The level of caspase-9 and the proapoptotic protein Bax was found to be significantly higher, while levels of the anti-apoptotic protein Bcl-2 were lower, in the pcDNA3.1-FN1 group compared with the blank and pcDNA3.1-NC groups. Compared with those in the control group, the level of caspase-9 and Bax was significantly higher, whereas that in Bcl-2 was lower in the PE group. Caspase-9 and Bax protein was significantly lower, while that of Bcl-2 was higher in the FN1-siRNA

group compared with the PE and NC-siRNA groups. These results suggested that overexpression of FN1 promoted apoptosis in HUVECs. By contrast, FN1 knockdown suppressed apoptosis in HUVECs that were treated with serum from patients with PE.

Effects of FN1 overexpression and knockdown on autophagy in HUVECs

It has been reported that the amount of LC3B is proportional to the number of autophagic vacuoles, and ATG5 and BECN1 also serve a critical role in autophagosome formation (Chen, *et al*.,2018). Therefore, western blotting was performed to measure the protein levels of autophagy markers LC3B, ATG5 and BECN1. Compared with the control group, the level of LC3B, ATG5, and BECN1 was increased in the PE group (Fig. 4B. Supplementary Fig. S3). Furthermore, the levels of LC3B, ATG5, and BECN1 were all significantly increased in the pcDNA3.1-FN1 group, compared with that in the pcDNA3.1-NC group. However the levels of LC3B, ATG5, and BECN1 were significantly reduced in the FN1-siRNA group, compared with those in the PE and NC-siRNA groups.

To determine the effect of pcDNA3.1-FN1 or FN1-siRNA on autophagic activity, the tandem fluorescence protein mCherry-GFP-LC3B was infected into HUVECs to detect autophagosome formation and autophagosome maturation into autolysosomes. Under a fluorescence microscope, autophagosomes were shown as yellow, representing the merge between green (green flourescent protein: GFP) and red

(mCherry) fluorescence. If fusion between autophagosomes and lysosomes occurs to generate autolysosomes, the orange or light red fluorescence would be exhibited owing to the weakening of green fluorescence in acidic pH (Shen, *et al*.,2019). As shown in Fig. 5, only a limited quantity of weak yellow signals were observed in the cytoplasm of HUVECs in the blank and control groups, suggesting a presence of a small number of autophagosomes and low autophagy level. In contrast, in the PE group the numbers of yellow and orange puncta increased compared with the blank and control groups. The results suggested that autophagy was activated and autophagic flux occurred in HUVECs following treatment with serum from patients with PE. In the pcDNA3.1-FN1 group, the numbers of both autophagosomes and autolysosomes, which fluoresce yellow and orange respectively, were increased compared with those in the pcDNA3.1-NC group, suggesting that autophagic activity was enhanced and autophagic flux was initiated following the upregulation of FN1. Meanwhile, compared with the NC-siRNA group, FN1-siRNA reduced the number and intensity of yellow and orange puncta, which represent autophagosomes and autolysosomes, respectively. These results indicated that overexpression of FN1 promoted the autophagic activity of HUVECs, but knockdown of FN1 inhibited the autophagic activity of HUVECs cultured with serum from patients with PE.

FN1 regulates apoptosis and autophagy in HUVECs through the PI3K/AKT/mTOR signaling pathway

Results from western blotting showed that mTOR and Akt phosphorylation were significantly decreased in the PE group compared with those in the control group (Fig. 6, Supplementary Fig. S4). Moreover, the levels of p-mTOR and p-Akt were significantly lower in the pcDNA3.1-FN1 group compared with those in the blank and pcDNA3.1-NC groups. However, mTOR and AKT phosphorylation in the FN1-siRNA group were markedly increased compared with those in the siRNA-NC and PE groups. These results suggested that overexpression of FN1 inhibited the PI3K/AKT/mTOR signaling pathway in HUVECs, while FN1-siRNA activated the PI3K/AKT/mTOR signaling pathway in HUVECs cultured with serum from patients with PE.

To explore whether FN1-siRNA inhibited apoptosis and autophagy by activating the PI3K/AKT/mTOR signaling pathway, LY294002, a PI3K inhibitor, was used to inhibit the activation of this pathway in the FN1-siRNA group. Subsequently, apoptosis, autophagy and the expression of related proteins were investigated. As depicted in Fig. 7 (Supplementary Fig. S5), the apoptotic rate was higher and the expression levels of caspase-9 and Bax were increased, while the expression of Bcl-2 was reduced, in the LY294002+FN1-siRNA group compared with those in the FN1-siRNA group. Meanwhile, compared with the FN1-siRNA group, the number of autophagosomes and autolysosomes, which fluoresce yellow and orange, respectively,

in the LY294002+FN1-siRNA group was found to be increased, indicating that the level of autophagy increased and autophagic flux occurred. Correspondingly, the expression of LC3B, ATG5, and BECN1 was increased in the LY294002+FN1-siRNA group compared with those in the FN1-siRNA group. These data demonstrated that LY294002 reversed the inhibitory effects of FN1-siRNA on apoptosis and autophagy in HUVECs cultured with serum from patients with PE.

Discussion

During PE, FN1 is synthesized by endothelial cells, smooth-muscle cells or fibroblasts in response to tissue injury (Gredmark, *et al*.,1999). Plasma FN1, which normally refers to soluble FN1 in the circulation, is released into the blood when endothelial injury occurs, as in pre-eclampsia. Cellular FN1 refers to FN1 that is secreted by cells *in vitro* or that can be found in the extracellular matrix surrounding tissues (Jones, *et al*.,1996). Elevated plasma FN1 may serve as an indicator of endothelial damage, which has been reported in a number of previous studies (Al-Yafeai, *et al*.,2018; Bodova, *et al*.,2011). In addition, it has been shown that maternal vascular endothelial injury is an accompanying pathological characteristic of pregnancy-induced hypertension syndrome, which can be predicted using the levels of plasma FN1 (Yang, *et al*.,2018; He, *et al*.,2015). Zhao, *et al*. (2017) indicated that change in plasma FN1 is a sensitive and specific predictor of PE, which can be used as a first-line screening tool for PE. The present study also provided evidence that the

level of plasma FN1 was elevated in the patients with PE, which was positively associated with the severity of PE, consistent with the results from the Zhao, *et al*. (2017) study. Meanwhile, the expression levels of FN1 in HUVECs grown in the presence of serum from patients with PE were also higher compare with those in the control, consistent with the results seen in patients in the present study.

Programmed cell death can be divided into two major types: apoptosis and autophagy. Apoptosis in particular, which is an evolutionarily conserved process, has been studied extensively (Losuwannarak, *et al*.,2018). Apoptosis and autophagy in endothelial cells are critically important during the development of PE. Li *et al*. (2013) suggested that the plasma from patients with PE could inhibit proliferation and promote apoptosis of HUVECs. Gao, *et al*. (2016) noted that the proliferation of HUVECs obtained from pregnant women with PE was significantly suppressed, which was accompanied by apoptosis. The present study also found that the apoptotic rate of HUVECs in the PE group was significantly higher compared with that in the control group, which is consistent with the aforementioned data. Furthermore, we demonstrated that overexpression of FN1 promoted the apoptosis of HUVECs, while silencing FN1 inhibited apoptosis in HUVECs cultured with serum from patients with PE. Apoptosis is typically determined by the ratio of anti-apoptotic protein Bcl-2 to proapoptotic protein Bax; in addition, as an initiator caspase, caspase-9 is also considered to be a central player in the apoptotic pathway (Cao, *et al*.,2019). Western blotting data verified further that treatment of HUVECs with serum from patients with PE or overexpression of FN1 upregulated the expression of caspase-9 and Bax, and

down-regulated Bcl-2. By contrast, FN1-siRNA significantly downregulated the expression of caspase-9 and Bax, but upregulated the expression of Bcl-2. These data suggest that overexpression of FN1 promoted HUVECs apoptosis, whereas knockdown of FN1 suppressed the apoptosis in HUVECs cultured with the serum from patients with PE.

Autophagy is a form of type-2 programmed cell death and is a conserved dynamic process used for the degradation and recycling of intracellular components (Qi, *et al*.,2018). Autophagy serves a critical role in cell survival, and alterations in autophagy are associated with a variety of diseases, such as cancer, and infectious and metabolic diseases (Levine, *et al*.,2011; Webster,2018). Compared with normotensive pregnant individuals, patients with hypertensive disease or PE exhibited significant autophagy activation, namely increased LC3B, and decreased p62 levels (Akaishi, *et al*.,2014; Nakashima, *et al*.,2017). Schaaf *et al*. (2019) implied that autophagy in endothelial cells played a vital role during prenatal vascular development. In consideration of the reported pivotal role of endothelial dysfunction in the pathogenesis of PE (Jiang,2016), we used the Ad-mCherry-GFP-LC3B to investigate autophagosome formation and its fusion with lysosomes in HUVECs. It was found that a small number autophagosomes were fused with lysosomes to generate autolysosomes, while autophagic flux occurred at a low level in HUVECs cultured with serum from patients with PE. Overexpression of FN1 increased the number of autophagosomes in HUVECs, but FN1-siRNA reduced the number of autophagosomes. ATG5 is essential for the formation of autophagosome by

promoting the lipidation of microtubule associated protein, whereas LC3Ⅱ is considered to be one of the key markers of autophagy (Doring, et al.,2018). Additionally, Beclin-1 (BECN1) is also well known as an important component for theinitiation of autophagosome formation during autophagy (Hamurcu, *et al*.,2019). In the present study, the protein levels of LC3B, ATG5, and BECN1 were detected by western blotting, the results of which concurred with those from our autophagosome formation experiments.

PI3K/AKT/mTOR is a major intracellular signaling pathway that is critical in the activation of numerous downstream effectors and is involved in cellular survival, proliferation and death (Kim,2017). The present study showed that overexpression of FN1 inhibited the phosphorylation of mTOR and Akt in HUVECs, which were increased in HUVECs cultured with serum from patients with PE after transfection with FN1-siRNA, suggesting that overexpression of FN1 inhibited PI3K/AKT/mTOR pathway activation, while knockdown of FN1 activated the PI3K/AKT/mTOR pathway. A rescue experiment was conducted using the PI3K inhibitor LY294002 to verify whether FN1 induced apoptosis and autophagy in HUVECs through the PI3K/AKT/mTOR signaling pathway. The results showed that LY294002 reversed the effects of FN1-siRNA on apoptosis and autophagy in HUVECs cultured with serum from patients with PE. Therefore, it is reasonable to suggest that FN1 facilitated apoptosis and autophagy in HUVECs cultured with serum from patients with PE through the PI3K/AKT/mTOR signaling pathway.

Conclusion

The present study found that FN1 was highly expressed in PE, and this expression may be closely associated with the pathogenesis of PE. *In vitro* experiments suggested that FN1 promoted apoptosis and autophagy in HUVECs by inhibiting the PI3K/AKT/mTOR signaling pathway, which may be the mechanism underlying its involvement in the pathogenesis of PE. These results may provide a new theoretical basis for the study of vascular endothelial cell injury and dysfunction, with the long-term goal of developing novel targets for the treatment of PE. However, the relation between FN1 and development of PE, in addition to its details of the mechanism(s) involved, require further exploration.

Data availability statement

The data underlying this article would be shared ton reasonable request to the corresponding author.

Authors' roles

All authors qualify for authorship by contributing substantially to this article. HW contributed to the conceptualization, funding acquisition, methodology, project administration and paper original draft; KL and JZ contributed to the formal analysis, data curation, investigation, validation and paper review & editing. All authors have

contributed to critical discussion, reviewed the final version of the article and approved it for publication.

Funding

This work was supported by a grant from the Science and Technology Department of Henan Province, China (No.192102310335).

Conflict of interest

The authors have no conflict of interest to declare.

References

ACOG Committee on Practice Bulletins-Obstetrics. ACOG practice bulletin. Diagnosis and management of preeclampsia and eclampsia.. Number 33, January 2002. *Obstet Gynecol* 2002; **99:** 159-67.

Akaishi R, Yamada T, Nakabayashi K, Nishihara H, Furuta I, Kojima T, Morikawa M, Yamada T, Fujita N, Minakami H. Autophagy in the placenta of women with hypertensive disorders in pregnancy. *Placenta* 2014; **35:** 974-980.

Ali SM, Khalil RA. Genetic, immune and vasoactive factors in the vascular dysfunction associated with hypertension in pregnancy. *Expert Opin Ther Targets* 2015; **19:** 1495-1515.

Al-Yafeai Z, Yurdagul AJ, Peretik JM, Alfaidi M, Murphy PA, Orr AW. Endothelial FN (Fibronectin) Deposition by alpha5beta1 Integrins Drives Atherogenic Inflammation. *Arterioscler Thromb Vasc Biol* 2018; **38:** 2601-2614.

Aydin T, Varol FG, Sayin NC. Third trimester maternal plasma total fibronectin levels in pregnancy-induced hypertension: results of a tertiary center. *Clin Appl Thromb Hemost* 2006; **12:** 33-39.

Bodova KB, Biringer K, Dokus K, Ivankova J, Stasko J, Danko J. Fibronectin, plasminogen activator inhibitor type 1 (PAI-1) and uterine artery Doppler velocimetry as markers of preeclampsia. *Dis Markers* 2011; **30:** 191-196.

400 Cao RJ, Li K, Xing WY, Du S, Li Q, Zhu XJ, Cui SS. Disabled-1 is down-regulated in clinical breast
401 cancer and regulates cell apoptosis through NF-kappaB/Bcl-2/caspase-9. *J Cell Mol Med* 2019; **23:**
402 1622-1627.

403 Chen J, Zhang L, Zhou H, Wang W, Luo Y, Yang H, Yi H. Inhibition of autophagy promotes
404 cisplatin-induced apoptotic cell death through Atg5 and Beclin 1 in A549 human lung cancer cells.
Mol Med Rep 2018; **17:** 6859-6865.

406 de Alwis N, Beard S, Mangwiro YT, Binder NK, Kaitu'U-Lino TJ, Brownfoot FC, Tong S, Hannan NJ.
407 Pravastatin as the statin of choice for reducing pre-eclampsia-associated endothelial dysfunction.
Pregnancy Hypertens 2020; **20:** 83-91.

409 Dogan E, Demir SC, Gulec UK. Maternal soluble vascular cytoplasmic adhesion molecule-1 and
410 fibronectin levels in early- and late-onset preeclamptic pregnancies. *Clin Exp Obstet Gynecol*
411 2014; **41:** 681-684.

412 Doring T, Zeyen L, Bartusch C, Prange R. Hepatitis B Virus Subverts the Autophagy Elongation
413 Complex Atg5-12/16L1 and Does Not Require Atg8/LC3 Lipidation for Viral Maturation. *J Virol*
414 2018; **92**.

415 Gao Q, Zhu X, Chen J, Mao C, Zhang L, Xu Z. Upregulation of P53 promoted G1 arrest and apoptosis
416 in human umbilical cord vein endothelial cells from preeclampsia. *J Hypertens* 2016; **34:**
417 1380-1388.

418 Gathiram P, Moodley J. Pre-eclampsia: its pathogenesis and pathophysiolgy. *Cardiovasc J Afr* 2016;
27: 71-78.

420 Gredmark T, Bergman B, Hellstrom L. Total fibronectin in maternal plasma as a predictor for
421 preeclampsia. *Gynecol Obstet Invest* 1999; **47:** 89-94.

422 Hamurcu Z, Delibasi N, Nalbantoglu U, Sener EF, Nurdinov N, Tasci B, Taheri S, Ozkul Y,
423 Donmez-Altuntas H, Canatan H et al. FOXM1 plays a role in autophagy by transcriptionally
424 regulating Beclin-1 and LC3 genes in human triple-negative breast cancer cells. *J Mol Med (Berl)*
425 2019; **97:** 491-508.

426 He P, Shao D, Ye M, Zhang G. Analysis of gene expression identifies candidate markers and pathways
427 in pre-eclampsia. *J Obstet Gynaecol* 2015; **35:** 578-584.

428 Jiang F. Autophagy in vascular endothelial cells. *Clin Exp Pharmacol Physiol* 2016; **43:** 1021-1028.

429 Jones I, Cowley D, Andersen M, Vacca A, Voroteliak V. Fibronectin as a predictor of preeclampsia: a
430 pilot study. *Aust N Z J Obstet Gynaecol* 1996; **36:** 1-3.

431 Kim GD. Myricetin Inhibits Angiogenesis by Inducing Apoptosis and Suppressing PI3K/Akt/mTOR
432 Signaling in Endothelial Cells. *J Cancer Prev* 2017; **22:** 219-227.

433 Levine B, Mizushima N, Virgin HW. Autophagy in immunity and inflammation. *Nature* 2011; **469:**
434 323-335.

435 Levy R. The role of apoptosis in preeclampsia. *Isr Med Assoc J* 2005; **7:** 178-181.

436 Li LX, Li XF, Zhang LL, Zhang Y, Guo RX, Zhang XY, Zhou Y, Qiao YH, Su K. [Effects of plasma
437 from patients with preeclampsia on the proliferation and apoptosis of human umbilical vein
438 endothelial cells and its relationship with lysophosphatidic acid receptors]. *Zhonghua Fu Chan Ke Za Zhi* 2013; **48:** 102-106.

440 Losuwannarak N, Sritularak B, Chanvorachote P. Cycloartobiloxanthone Induces Human Lung Cancer
441 Cell Apoptosis via Mitochondria-dependent Apoptotic Pathway. *In Vivo* 2018; **32:** 71-78.

442 Monte F, Awad KR, Ahuja N, Kim H, Aswath P, Brotto M, Varanasi VG. Amorphous Silicon
443 Oxynitrophosphide-Coated Implants Boost Angiogenic Activity of Endothelial Cells. *Tissue Eng Part A* 2020; **26:** 15-27.

445 Nakashima A, Aoki A, Kusabiraki T, Cheng SB, Sharma S, Saito S. Autophagy regulation in
446 preeclampsia: Pros and cons. *J Reprod Immunol* 2017; **123:** 17-23.

447 Osol G, Ko NL, Mandala M. Altered Endothelial Nitric Oxide Signaling as a Paradigm for Maternal
448 Vascular Maladaptation in Preeclampsia. *Curr Hypertens Rep* 2017; **19:** 82.

449 Qi QM, Xue YC, Lv J, Sun D, Du JX, Cai SQ, Li YH, Gu TC, Wang MB. Ginkgolic acids induce
450 HepG2 cell death via a combination of apoptosis, autophagy and the mitochondrial pathway. *Oncol Lett* 2018; **15:** 6400-6408.

452 Rana S, Lemoine E, Granger JP, Karumanchi SA. Preeclampsia: Pathophysiology, Challenges, and
453 Perspectives. *Circ Res* 2019; **124:** 1094-1112.

454 Schaaf MB, Houbaert D, Mece O, Agostinis P. Autophagy in endothelial cells and tumor angiogenesis. *Cell Death Differ* 2019; **26:** 665-679.

456 Shen Y, Zhou N, An J, Zhang J, Wang M, Li Y, Jiang P. Haemophilus parasuis infection in 3D4/21
457 cells induces autophagy through the AMPK pathway. *Cell Microbiol* 2019; **21:** e13031.

458 Speziale P, Arciola CR, Pietrocola G. Fibronectin and Its Role in Human Infective Diseases. *Cells*
459 2019; **8:** 1516.

460 To WS, Midwood KS. Plasma and cellular fibronectin: distinct and independent functions during tissue
461 repair. *Fibrogenesis Tissue Repair* 2011; **4:** 21.

462 Tranquilli AL, Dekker G, Magee L, Roberts J, Sibai BM, Steyn W, Zeeman GG, Brown MA. The
463 classification, diagnosis and management of the hypertensive disorders of pregnancy: A revised
464 statement from the ISSHP. *Pregnancy Hypertens* 2014; **4:** 97-104.

465 Webster JD. Multifaceted Roles of Autophagy in Health and Disease. *Vet Pathol* 2018; **55:** 361-362.

466 Witcher PM. Preeclampsia: Acute Complications and Management Priorities. *AACN Adv Crit Care*
467 2018; **29:** 316-326.

468 Yang TL, Lee PL, Lee DY, Wang WL, Wei SY, Lee CI, Chiu JJ. Differential regulations of fibronectin
469 and laminin in Smad2 activation in vascular endothelial cells in response to disturbed flow. *J*
Biomed Sci 2018; **25:** 1.

471 Yokomizo A, Takakura M, Kanai Y, Sakuma T, Matsubara J, Honda K, Naito S, Yamada T, Ono M.
472 Use of quantitative shotgun proteomics to identify fibronectin 1 as a potential plasma biomarker for
473 clear cell carcinoma of the kidney. *Cancer Biomark* 2011; **10:** 175-183.

474 Zhao J, Peng W, Ran Y, Ge H, Zhang C, Zou H, Ding Y, Qi H. Dysregulated expression of ACTN4
475 contributes to endothelial cell injury via the activation of the p38-MAPK/p53 apoptosis pathway in
476 preeclampsia. *J Physiol Biochem* 2019; **75:** 475-487.

477 Zhao M, Li L, Yang X, Cui J, Li H. FN1, FOS, and ITGA5 induce preeclampsia: Abnormal expression
478 and methylation. *Hypertens Pregnancy* 2017; **36:** 302-309.

Figure legends

Figure 1 Levels of plasma FN1, measured by ELISA, in different groups of women.

A: Levels of plasma fibronectin 1 (FN1) in patients with pre-eclampsia (PE) (n=80) and healthy pregnant women (n=40), ***P*<0.01, compared with the control group; B: Levels of plasma FN1 in pregnant women with MP (n=48) and SP groups (n=32). Values are shown as mean±SD. Student's *t*-test was used for statistical analysis. **P*<0.05, *versus* SP group.

MP: mild pre-eclampsia; SP: severe pre-eclampsia.

Figure 2 The morphology of HUVECs and expression of FN1 assessed by RT-qPCR and western blotting in HUVECs.

A: The morphology of human umbilical vein endothelial cells (HUVECs) was observed under the microscope. Scale bar: 50μm. B: The expression level of FN1 mRNA was detected by quantitative RT-PCR (RT-qPCR); C: Relative level of FN1 protein in HUVECs was detected by western blotting (Supplementary Fig. S1 shows the uncropped western blot). Values are shown as mean±SD, n=3. Student's *t*-test was used for statistical analysis. Different letters denote significant differences between groups. ^{a}P<0.05, *versus* blank group; ^{b}P<0.05, *versus* pcDNA3.1-NC group; ^{c}P<0.05, *versus* control group; ^{d}P<0.05, *versus* PE group; ^{e}P<0.05, *versus* NC-siRNA group. NC: negative control

Figure 3 Apoptosis in HUVECs in each group was detected by TUNEL assay.

Cells were observed using a fluorescence microscope. Nuclei were stained with DAPI and apoptotic cells were stained with red-blue fluorescence. Representative data are shown.

n=3, Scale bar=50μm.

Figure 4 The analysis of apoptosis-related proteins and autophagy marker proteins by western blotting.

A: Western blotting of apoptosis-related protein expression (also Supplementary Fig. S2); B: Western blotting of autophagy marker proteins LC3B, ATG5 and BECN1 (also Supplementary Fig. S3). Values are shown as mean±SD, n=3. Student's *t*-test was used for statistical analysis. Different letters denote significant differences between groups. [a]$P<0.05$, *versus* blank group; [b]$P<0.05$, *versus* pcDNA3.1-NC group; [c]$P<0.05$, *versus* control group; [d]$P<0.05$, *versus* PE group; [e]$P<0.05$, *versus* NC-siRNA group.

LC3B: microtubule associated protein 1 light chain 3 beta; ATG5: autophagy related gene 5; BECN1: Beclin-1.

Figure 5 Autophagosomes were detected by Ad-mCherry-GFP-LC3B labeling in HUVECs.

Adenovirus expression mCherry-green fluorescent proteins-LC3B fusion protein (Ad-mCherry-GFP-LC3B) was used to infect HUVECs. Cells were observed using a confocal microscope. Representative data are shown. Autophagosomes are shown as yellow, representing the merge between green flourescent protein (GFP) and red (mCherry) fluorescence. Autolysosomes are shown as orange or light red fluorescence. n=3, Scale bar=10μm.

Figure 6 The analysis of AKT, p-AKT, mTOR and p-mTOR levels in HUVECs by western blotting.

Level of AKT, p-AKT, mTOR and p-mTOR in HUVECs was detected by western blotting (also Supplementary Fig. S4). Values are shown as mean±SD, n=3. Student's *t*-test was used for statistical analysis. Different letters denote significant differences between groups. [a]$P<0.05$, *versus* blank group; [b]$P<0.05$, *versus* pcDNA3.1-NC group; [c]$P<0.05$, *versus* control group; [d]$P<0.05$, *versus* PE group; [e]$P<0.05$, *versus* NC-siRNA group; [f]$P<0.05$, *versus* FN1-siRNA group.

AKT: protein kinase B; p-AKT: AKT with phospho T308; mTOR: mechanistic target of rapamycin; p-mTOR: mTOR with phospho S2448

Figure 7 LY294002 reversed the inhibition of FN1-siRNA on apoptosis and autophagy in HUVECs.

A: Apoptosis rates were detected by TUNEL assay. Cells were observed using a fluorescence microscope. Apoptotic cells were stained with TUNEL (red) and nuclei were stained with DAPI. Scale bar=50μm, n=3. B: Autophagosomes were detected by Ad-mCherry-GFP-LC3B labeling. Cells were observed using a confocal microscope. Representative data are shown. Autophagosomes are shown as yellow, representing the merge between green fluorescence and red (mCherry) fluorescence. Autolysosomes are shown as orange or light red fluorescence. Scale bar=10μm, n=3. C: The levels of apoptosis marker proteins and autophagy marker proteins were analyzed by western blotting (also Supplementary Fig. S5). Values are shown as mean±SD, n=3. Student's t-test was used for statistical analysis. $^{a}P<0.05$, *versus* FN1-siRNA group.

Table I Clinical data for the control, MP and SP groups.

	Control group (n=40)	MP group (n=48)	SP group (n=32)	*P*-value
Age (years)	30.20±4.84	30.54±4.04	30.16±4.56	0.909
Gestational age at enrollment (weeks)	27.75±3.39	28.02±2.80	28.06±2.36	0.876
BMI (kg/m^2)	24.39±2.31	24.20±2.41	23.51±2.82	0.306
SBP (mmHg)	112.68±7.57	148.23±9.63[a]	152.21±14.34[a]	< 0.001
DBP (mmHg)	80.87±6.90	100.53±11.13[a]	101.51±10.49[a]	< 0.001
24h urine protein (g)	0.13±0.05	0.49±0.49[a]	1.29±1.22[ab]	< 0.001
Gestational age at birth (weeks)	38.30±1.31	37.41±2.65	30.34±2.62[ab]	< 0.001

[a]*P*<0.05, *versus* control group; [b]*P*<0.05, *versus* MP group. Multiple group comparisons were analyzed using ANOVA, followed by a least significant difference *t* test. All data are shown as mean±SD. MP, mild pre-eclampsia; SP, severe pre-eclampsia; SBP, systolic blood pressure; DBP, diastolic blood pressure.

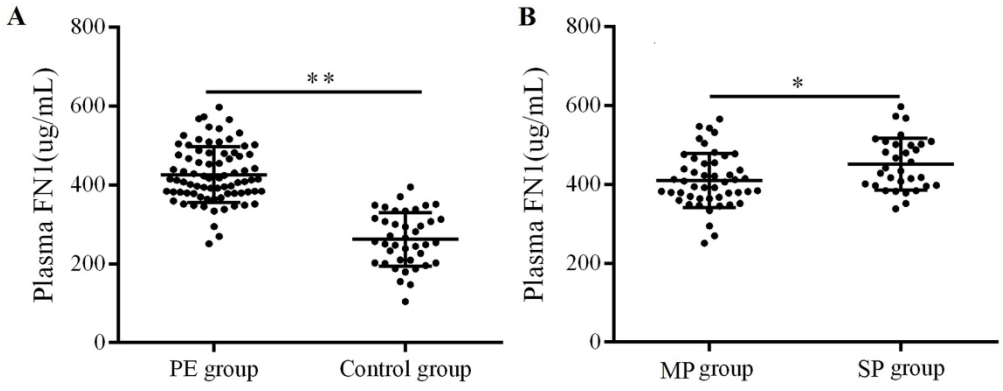

Figure 1

149x56mm (600 x 600 DPI)

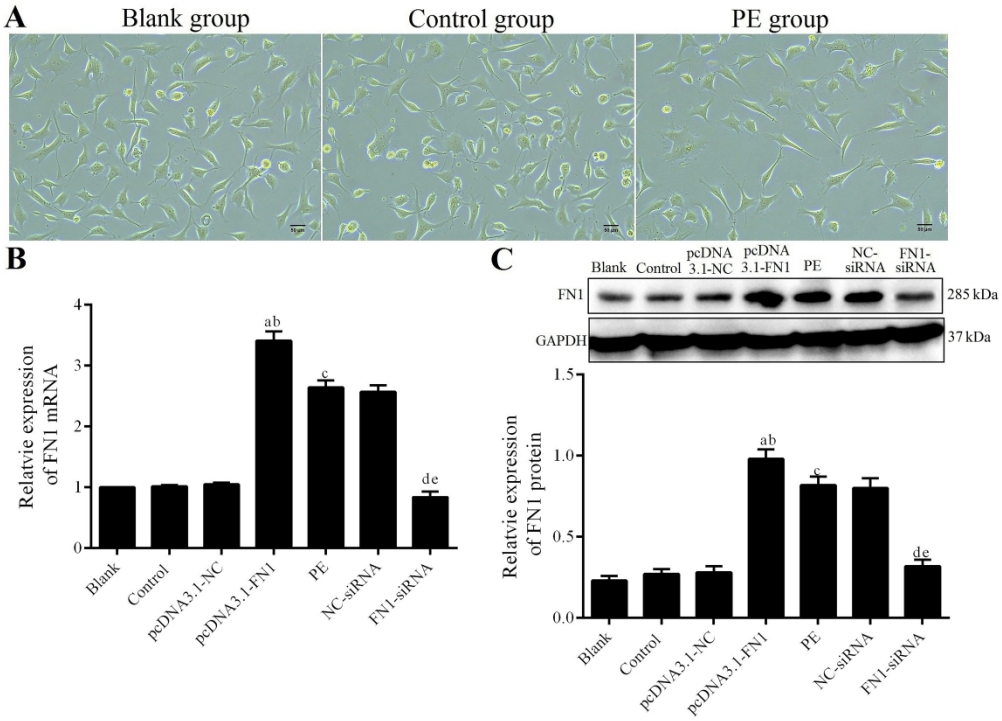

Figure 2

265x192mm (600 x 600 DPI)

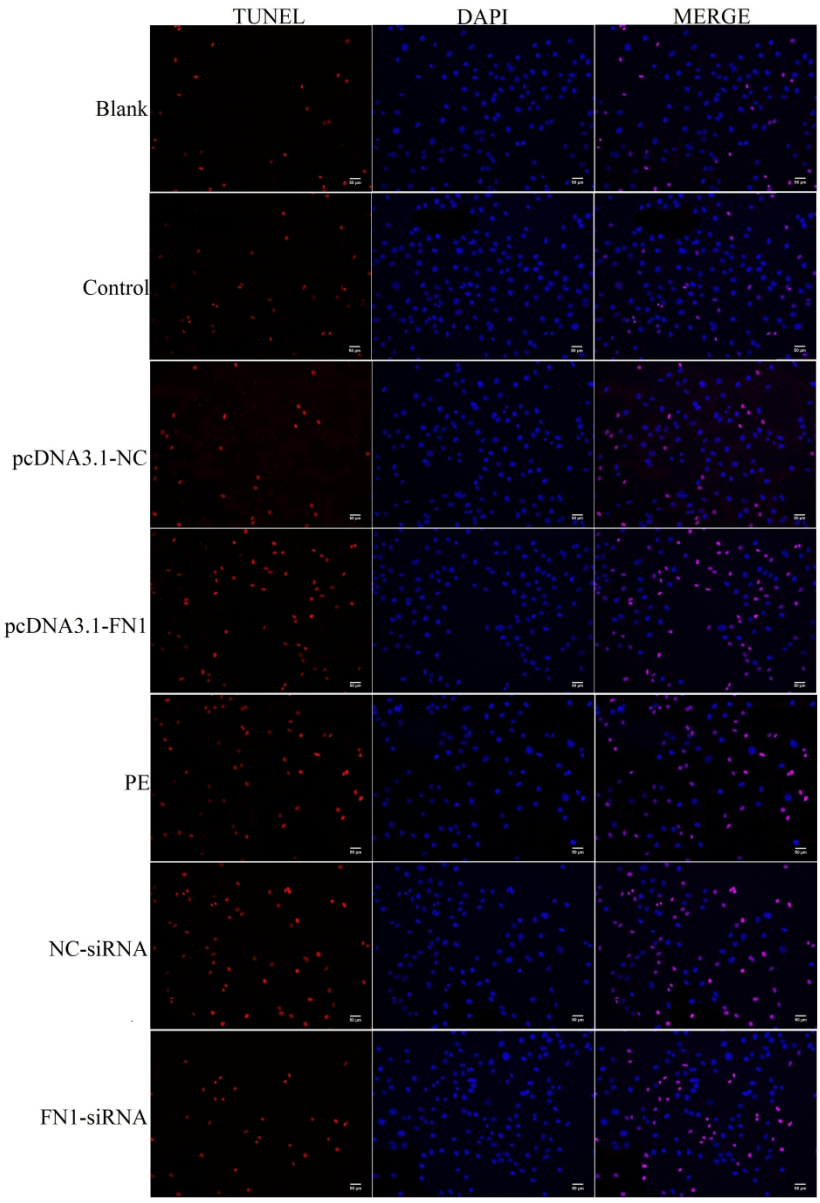

Figure 3

211x307mm (600 x 600 DPI)

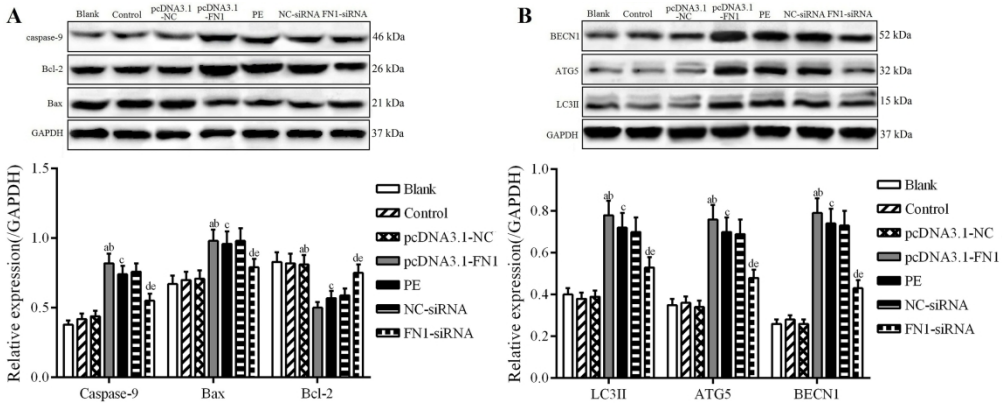

243x97mm (300 x 300 DPI)

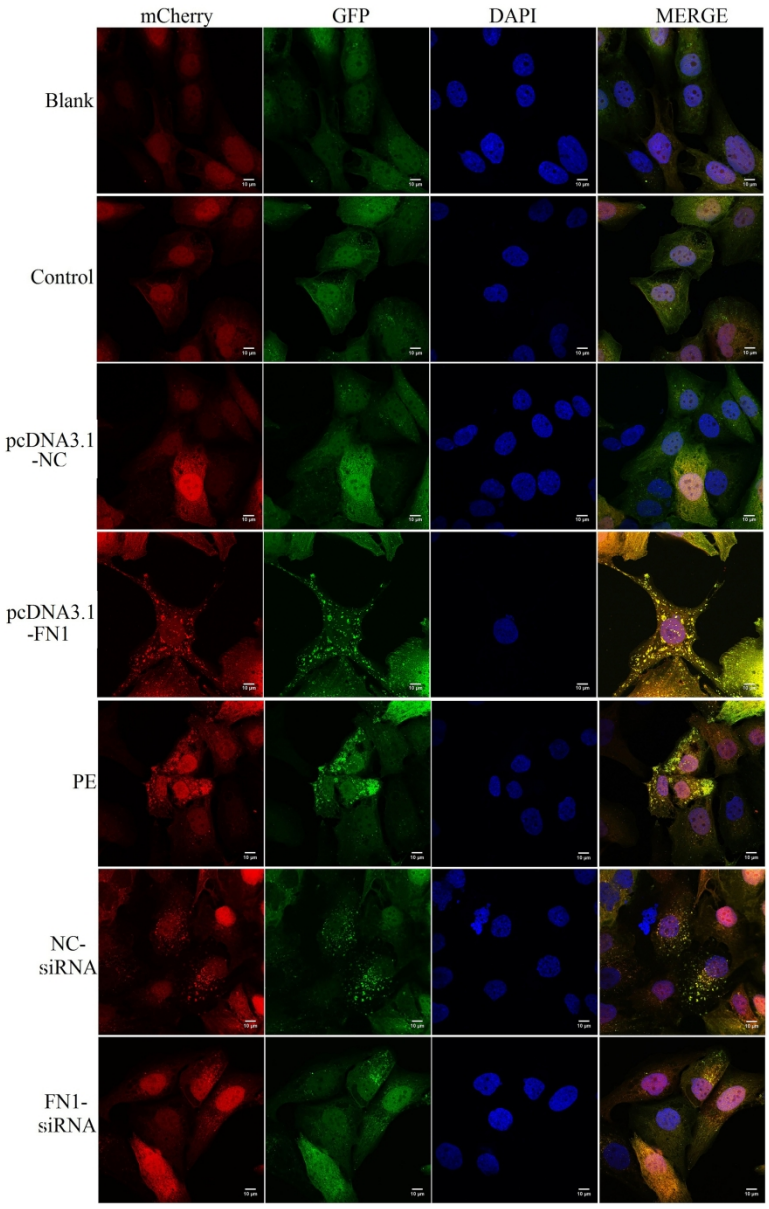

211x331mm (300 x 300 DPI)

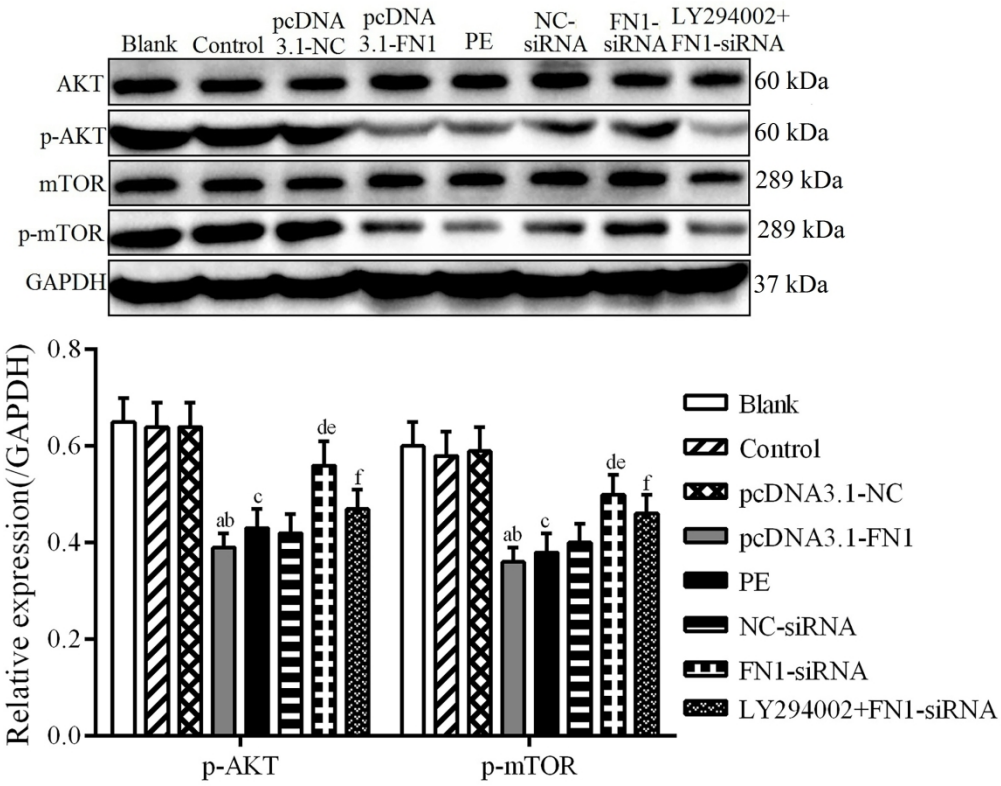

Figure 6

131x104mm (600 x 600 DPI)

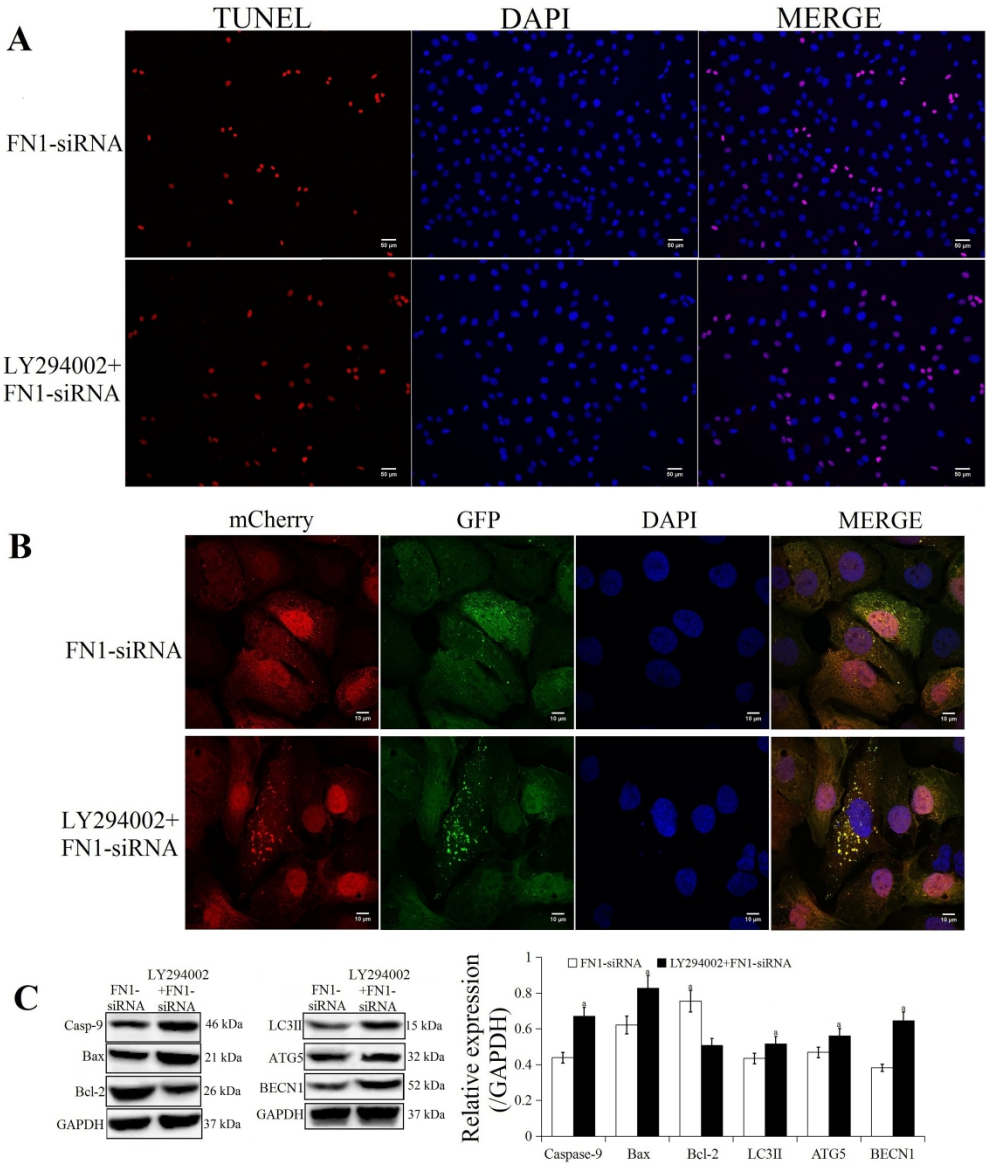

Figure 7

211x253mm (600 x 600 DPI)